Materials Research Letters

ISSN: (Print) 2166-3831 (Online) Journal homepage: http://www.tandfonline.com/loi/tmrl20

Stability of suspended monolayer graphene membranes in alkaline environment

A. Miranda & A. Lorke

To cite this article: A. Miranda & A. Lorke (2018) Stability of suspended monolayer graphene membranes in alkaline environment, Materials Research Letters, 6:1, 49-54, DOI: 10.1080/21663831.2017.1390793

To link to this article: http://dx.doi.org/10.1080/21663831.2017.1390793

MATER. RES. LETT., 2017
VOL. 6, NO. 1, 49–54
https://doi.org/10.1080/21663831.2017.1390793

MATERIALS RESEARCH LETTERS
Taylor & Francis
Taylor & Francis Group

ORIGINAL REPORT

OPEN ACCESS Check for updates

Stability of suspended monolayer graphene membranes in alkaline environment

A. Miranda[a,b] and A. Lorke[a]

[a]Department of Physics and CENIDE, Universität Duisburg-Essen, Duisburg, Germany; [b]Institute of Physics, Ecole Polytechnique Fédérale de Lausanne (EPFL), Lausanne, Switzerland

ABSTRACT

We report on the structural, chemical and electrical compatibility of graphene in an alkaline environment, namely diluted KOH solutions as those used in standard nanofabrication methods. Electron microscopy and Raman spectroscopy indicate that graphene preserves its structural properties during the process. The electrical transport properties such as conductance and shape of the Dirac point, appear degraded after KOH treatment, but can be fully recovered by current annealing. Electron beam-induced etching can provide further nanofabrication subsequent to KOH processing. These results demonstrate that, with the due precautions, graphene-based structures can be integrated in standard fabrication processes involving KOH.

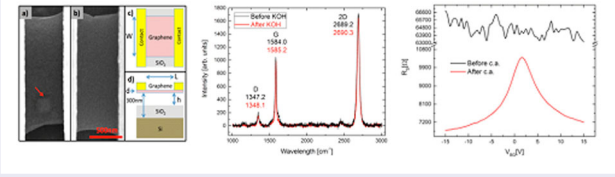

IMPACT STATEMENT

To be implemented in novel (nano) devices, graphene must be compatible with standard fabrication techniques. We show how graphene's intrinsic properties can be restored after exposure to an alkaline environment.

ARTICLE HISTORY
Received 20 June 2017

KEYWORDS
Graphene; KOH; EBIE; alkaline; current annealing

Since the isolation of monolayer graphene [1] there has been a great research interest in uncovering the physical properties of this two-dimensional system. In particular its remarkable electronic properties [2–4] make it a candidate for the next generation electronic nanotechnology. Suspended graphene has peculiar properties compared to supported graphene, such as a higher electrical [5] and thermal conductivity [6–8], mechanical elasticity [9–11] and sensitivity to gases [12]. Therefore it has found specific applications, e.g. in resonators [13–15], gas sensors [16], M/NEMS [17,18], pressure drums [19] or ballistic nanodevices [20,21] to name a few.

A relevant aspect for the application of both supported and suspended graphene as a component in modern electronic devices or M/NEMS is the possibility to integrate it with both well-established technologies, namely Si-technology, and more recently developed ones such as flexible electronics [22,23]. As such it is important to assess the chemical and physical compatibility of graphene to the fabrication steps involved in these technologies. Concerning chemical processes, for instance, graphene has shown very high stability after immersion in both pure and buffered HF (BOE),[1] while, as a pure layer of carbon, it is damaged by immersion in sulfuric acid, or so-called piranha etchants.

Potassium hydroxide (KOH) is commonly used as an agent to etch silicon [24–26], and was recently applied as an etchant for flexible substrates such as PDMS [27–29].

It is thus of interest to study the interaction of KOH with graphene in order to assess the compatibility of KOH-based processes with graphene-based devices. Previous studies on KOH interaction with graphene were limited to its role as an electrolyte [30–32] as well as an agent for chemical modification of graphene [33] for supercapacitive applications, or as a processing step to remove graphene from SiO_2 [34,35]. However a

CONTACT A. Miranda alessio.miranda@epfl.ch Department of Physics, Universität Duisburg-Essen, Duisburg 47058, Germany; Institute of Physics, Ecole Polytechnique Fédérale de Lausanne (EPFL), Lausanne CH-1015, Switzerland

Supplemental data for this article can be accessed here. https://doi.org/10.1080/21663831.2017.1390793

comprehensive study on the interaction of KOH processing on the structural and electrical properties of micron-sized single layer flakes is missing. In this paper we present an investigation of the modification of the structural and electrical properties of suspended graphene microribbons after immersion in a KOH solution and successive rinsing in water.

Commercially purchased chemical vapor deposition (CVD) graphene[2] deposited on a 300 nm Si/SiO_2 substrate was patterned into microribbons (2.5 µm × 20 µm) using optical lithography, followed by O_2 plasma ashing. The microribbons were contacted using standard electron beam lithography and metal deposition (Ti/Au 5/120 nm) followed by lift-off in acetone [36]. A second electron beam lithography step was used to create a rectangular opening in PMMA around the patterned graphene. This opening serves as a mask for under-etching the SiO_2 and thus create an electrically contacted, suspended strip of graphene [37,38].

The under-etching was achieved by immersing the sample in buffered HF, followed by rinsing in water at room temperature (RT). The samples were then immersed in a 5–20% water-diluted KOH solution at RT to 60°C, for 1–3 minutes. In order to remove the PMMA mask, the samples were transferred in semiconductor grade acetone for 5–10 minutes, and isopropyl alcohol (IPA) for 5 minutes at the same temperature of the KOH solution. After a final rinsing for 5 to 10 minutes in deionized water at the same temperature as previous solvents, the samples were finally transferred to hot IPA (60°C). This solution is allowed to evaporate, and the low-surface tension of warm isopropanol ensures that capillary forces do not crack the suspended graphene devices during evaporation.

SEM pictures of graphene microribbons, suspended over Si (Figure 1(a)) and SiO_2 (Figure 1(b)) after processing in KOH show that in both cases the overall process does not cause visible structural damages or deformation in the graphene flakes.

Figure 1(c,d)[3] show schematically the top and cross-sectional view of the suspended graphene device we fabricated: W, and L are the width and length of the suspended graphene between the two contacts, and h is the thickness of the removed SiO_2 after exposure to buffered HF, and d is the thickness of graphene [5] $d = 0.33$ nm.

All devices exhibit similar results in the investigated range of parameters (temperature, KOH concentration, immersion time . . .).

To investigate further the structural modification of samples during KOH treatment, Raman spectroscopy was performed on the sample using a commercial set-up at the intermediate stage of the process, i.e. immediately after suspension, before immersion in KOH, and at the final stage, after exposure to KOH. The Raman spectra of suspended microribbons with and without KOH treatment are shown in Figure 2. The spectra were taken at the same nominal conditions and on the same position of a suspended graphene microribbon using a laser at a wavelength of 532 nm as a source and a spectrometer with 2400 l/mm. The characteristic Raman peaks [39] D, G and $2D$ (also called G') of graphene are clearly visible in both the spectra. For a better evaluation of the figure, the intensity of the spectra has been normalized so that the intensity of the G peak is equal to $I(G) = 1000$ in both spectra.

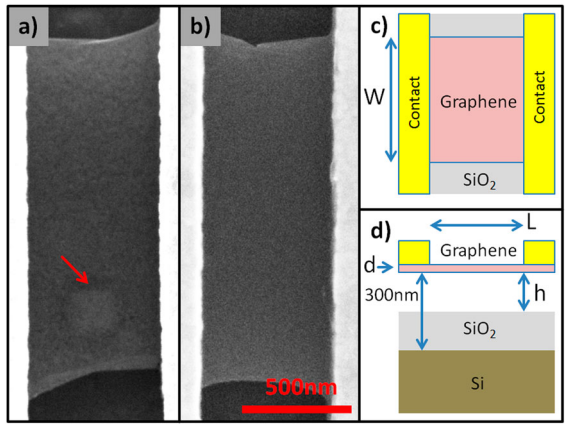

Figure 1. Graphene microribbons suspended on Si (a) and SiO_2 (b) substrates after immersion in KOH, showing its structural stability. In (a), the arrow indicate a probable pyramidal shape of KOH-etched silicon visible through the graphene layer, the folded edges are due to the suspension process, and not related to the KOH treatment. (c) top and (d) cross-sectional schematic view of a generic suspended graphene device. W, L, d are the width, length and thickness of the suspended graphene between the two contacts, and h is the thickness of removed SiO_2 after etching in BOE.

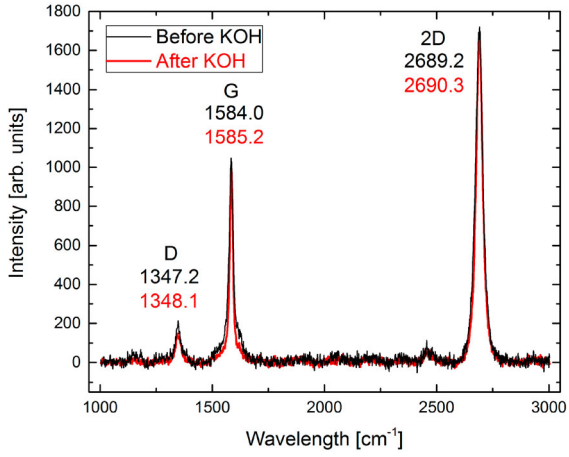

Figure 2. Raman spectra of a suspended graphene nanoribbon device, before (black) and after (red) immersion in KOH. Numbers correspond to the positions of the centers of the peaks.

Table 1. Evaluation of positions, FWHM, and intensities of the *D*, *G* and 2*D* peaks before and after immersion in KOH.

	Pos(*D*) [cm^{-1}]	FWHM(*D*) [cm^{-1}]	I(*D*) [a.u.]	Pos(*G*) [cm^{-1}]	FWHM(*G*) [cm^{-1}]	*I*(*G*) [a.u.]	Pos(2*D*) [cm^{-1}]	FWHM(2*D*) [cm^{-1}]	*I*(2*D*) [a.u.]
Before KOH	1347.2	23.4	182	1584	20.8	1000	2689.2	40.3	1828
After KOH	1348.1	33.2	163	1585.2	15.7	1000	2690.3	34.6	1781

Table 1 shows the numerical values of the principal peaks of the spectra shown in Figure 2. The position, full width half maximum (FWHM) and intensity of the peaks were calculated by fitting the experimental data with single Lorentzian curves. The ratio between the intensity of the 2*D* and *G* peak $I(2D)/I(G)$ is about 1.81 ± 002, indicating that graphene conserves its structural properties [39] after immersion in KOH. Both the position of the *G* and 2*D* peaks show a modest blueshift of 1.1 cm^{-1} after KOH treatment, which suggests a slight residual *p*-doping [40] as also confirmed by the reduction of the FWHM of the *G* peak after immersion.

The ratio between the intensities *G* and *D* peak is around $I(G)/I(D) = 5.5$ before and $I(G)/I(D) = 6.1$ after KOH, while the FWHM of the *D* peak increases by 42% after KOH treatment. By applying a recent version of the Tuinstra and Koenig model [41], we can estimate the crystallite graphene size as $L(\text{nm}) = (2.4 \times 10^{-10})\lambda^4_{\text{laser}}(I_G/I_D)$ to be 107 and 118 nm, respectively. We explain the increase in crystallite size by the fact that the *D* peak is highly edge sensitive [42], and residual KOH might fill vacancies or gaps in the defective structure of suspended graphene, but further studies would be necessary for a better understanding of the phenomenon.

In order to establish the effect of immersion of KOH on the electrical properties of suspended graphene, we bonded a suspended sample after full treatment in KOH solution to a chip carrier and inserted it in an SEM with external electrical connections. This system has the advantage that SEM pictures can be taken *in situ* at any time before, during or after measurement while keeping the sample at the measurement conditions. The electrical measurements took place at RT and at a pressure of $P = 5 \times 10^{-7}$ mBar. A constant potential difference (source drain voltage) of $V_{\text{SD}} = 100$ mV was applied between the two contacts holding the suspended graphene device, while a backgate voltage applied to the conductive Si substrate was swept in the range $-15\text{V} \leq V_{\text{BG}} \leq +15\text{V}$. The black curve in Figure 3(a) shows the resistance as a function of the backgate voltage of the KOH-treated sample. The sheet resistance is high, and the Dirac neutrality point is not visible in the explored backgate voltage range. This is due to the presence of residuals and impurities on the surface of graphene, which act as scatterers and degrade the conductance [43,44]. In order to improve the electrical properties of graphene, we performed current annealing [45], that is the application of a controlled large

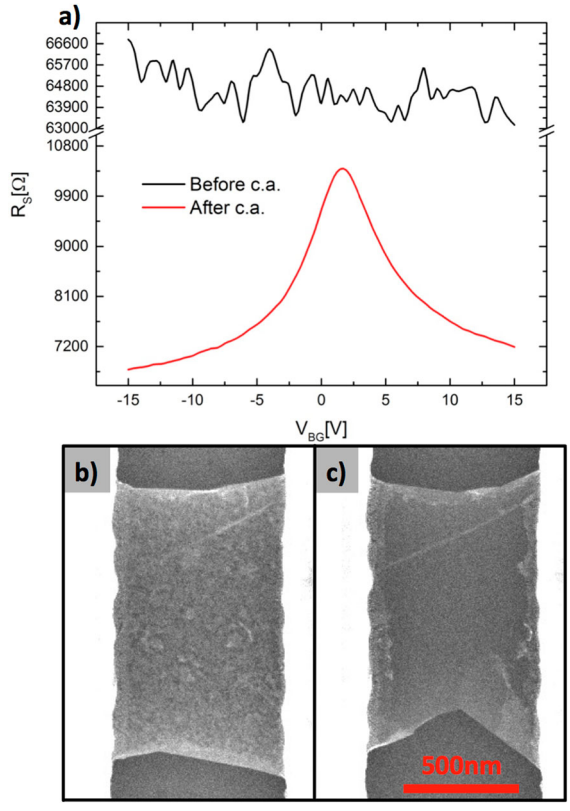

Figure 3. (a) Electrical measurements of the sheet resistance as a function of the backgate voltage ($V_{\text{SD}} = 100$ mV, $V_{\text{BG}} = \pm 15$V) for a suspended graphene microribbon treated with KOH, before and after current annealing. (b) and (c): images of the measured suspended graphene device before (b) and after (c) current annealing. The surface of suspended graphene appears cleaner after current annealing.

current to recover its electrical properties. In our case, we applied an increasing source drain voltage in steps of $\Delta V_{\text{SD}} = 100$ mV and monitored the evolution of the device resistance: after each step we waited for the resistance to stabilize and then increased the applied voltage; the annealing process was completed, when successive steps did not show a significant change in resistance. For this device, we increased the voltage up to $V_{\text{SD}} = 3.2$V, after which we noticed that the resistance did not decrease any further, a hint that current annealing was complete. This voltage corresponds to a current of $I = 590\,\mu$A and a power $P = 1.9$ mW.

The electrical measurements of the resistance of the same sample after current annealing are shown as the red curve in Figure 3(a). Now a well-centered Dirac point with a sheet resistance of the same order of magnitude

as in pristine graphene [3] is observable. This is due to the fact that current annealing removes effectively the KOH residues and other impurities from the surface of suspended graphene, as shown by the SEM images of the measured flake before (Figure 3(b)) and after (Figure 3(c)) current annealing. In Figure 3(c) it can be observed that current annealing was pushed a bit too much and the graphene layer started to crack at the edges [46].

Characteristic electronic parameters of the cleaned graphene device, such as contact resistance R_{cont}, mobility μ, and residual carrier concentration n_0 can be extrapolated by fitting [47] the gate-dependent resistance data with the formula:

$$R_{\text{tot}} = R_{\text{cont}} + R_{\text{chan}} = R_{\text{cont}} + (N_{\text{sq}}/e\mu n_{\text{tot}}),$$

where R_{chan} is the resistance of the graphene channel region, N_{sq} the length-to-width ratio (number of squares) of the graphene device, e the charge of electron, and n_{tot} the carrier density in the graphene channel region. The latter can be expressed as $n_{\text{tot}} = \sqrt{n_0^2 + n_{\text{BG}}^2}$ that is the combination of n_0, which is the residual carrier densities generated by defects and charge impurities, which are present in non-ideal graphene, and the voltage dependent carrier density given by $n_{\text{BG}} = (C_{\text{eq}}/e)(V_{\text{BG}} - V_{\text{Dirac}})$. The equivalent capacitance C_{eq} is calculated as the series of the two capacitors $C_{\text{eq}} = (h/\epsilon_0 + (d_{SiO_2} - h)/\epsilon_0\epsilon_{SiO_2})^{-1}$, representing the etched layer (thickness h) and the remaining SiO_2 layer (thickness d_{SiO_2}) between graphene and the Si backgate. Applying the fitting to the electrical measurements of the cleaned graphene device, for which $h = 115$ nm, and $N_{\text{sq}} = 0.73$, we extrapolate $\mu = 3800\,\text{cm}^2/\text{Vs}$, $R_{\text{cont}} = 4600\Omega$, and $n_0 = 4.1 \times 10^{11}\,\text{cm}^{-2}$.

These values are comparable with those of reference samples, which were fabricated from the same CVD graphene and with the same fabrication and annealing conditions, but without the immersion in KOH. Thus, the low value of mobility and the high value of impurity carriers compared to the best suspended graphene samples [5], should be attributed to the overall quality of processed CVD graphene, and not to the immersion in KOH.

Finally, we show that suspended graphene, after being treated after KOH processing, can still be directly patterned using resist free nanofabrication techniques such as water assisted electron beam-induced etching (EBIE) [37]. EBIE is a technique based on the selective etching of graphene by selectively irradiating parts of the sample with a focused electron beam in the presence of a water vapor environment. The combined effect of the electron beam and vapor adsorbate on graphene induces a chemical reaction which etches the irradiated parts of suspended graphene with a resolution of 7 nm [37]. To pattern the samples using this technique, we used an acceleration voltage $V = 30$ kV, a current $I = 0.69$ nA and a dose $D = 10\,\mu\text{C}/\mu\text{m}^2$. This dose is higher than the one needed for pristine suspended graphene, ($4\,\mu\text{C}/\mu\text{m}^2$), because KOH residue forms a protective layer on the surface of graphene. Figure 4 shows the successful patterning of nanoscopic structures such as nanoribbons (a), asymmetric constrictions (b), and quantum dots (c). Interestingly, after immersion in KOH, graphene acquires a remarkable stiffness, and after the cut, graphene remains suspended, even when attached to only one contact (see Figure 4(a)).

In summary, we have shown that suspended graphene is structurally stable after immersion in a KOH solution and subsequent rinsing in water. The Raman spectra before and after immersion show that the structural properties of graphene are preserved, apart from a limited residual doping. Residual contamination of KOH degrades the electrical properties of graphene with respect to pristine conditions, causing a high-sheet resistance, and disappearance of the Dirac point, however, intrinsic conditions can be fully recovered by current annealing. Furthermore, suspended graphene covered with a residual layer of KOH can be efficiently patterned by EBIE with nanometric precision, providing an additional possibility to subsequent nanofabrication.

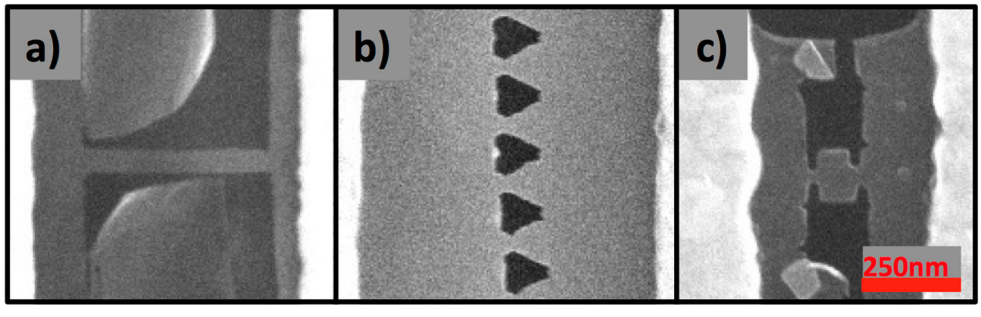

Figure 4. Patterned suspended graphene after KOH process using water assisted EBIE: suspended nanoribbons (a), asymmetric constrictions (b), and quantum dots (c).

Notes

1. BOE 7:1 (34.8% NH_4F, 6.5% HF, 58.7% H_2O).
2. Graphene Supermarket.
3. Details of the specific fabrication process for the devices shown in each figure can be found in the supplementary information.

Acknowledgements

The authors would like to thank Jens Theis, Mathias Bartsch and Martin Paul Geller for fruitful discussions and support.

Disclosure statement

No potential conflict of interest was reported by the authors.

References

[1] Novoselov KS, Geim AK, Morozov SV, et al. Electric field effect in atomically thin carbon films. Science. 2004;306(5696):666–669.
[2] Castro Neto AH, Guinea F, Peres NMR, et al. The electronic properties of graphene. Rev Mod Phys. 2009;81(1):109–162.
[3] Geim AK, Novoselov KS. The rise of graphene. Nat Mater. 2007;6(3):183–191.
[4] Katsnelson MI. Graphene: carbon in two dimensions. Mater Today. 2007;10(1):20–27.
[5] Bolotin KI, Sikes KJ, Jiang Z, et al. Ultrahigh electron mobility in suspended graphene. Solid State Commun. 2008;146(9–10):351–355.
[6] Chen S, Moore AL, Cai W, et al. Raman measurements of thermal transport in suspended monolayer graphene of variable sizes in vacuum and gaseous environments. ACS Nano. 2011;5(1):321–328.
[7] Lee J-U, Yoon D, Kim H, et al. Thermal conductivity of suspended pristine graphene measured by Raman spectroscopy. Phys Rev B. 2011;83(8):081419.
[8] Cai W, Moore AL, Zhu Y, et al. Thermal transport in suspended and supported monolayer graphene grown by chemical vapor deposition. Nano Lett. 2010;10(5):1645–1651.
[9] Lau CN, Bao W, Velasco J. Properties of suspended graphene membranes. Mater Today. 2012;15(6):238–245.
[10] Lee C, Wei X, Kysar JW, et al. Measurement of the elastic properties and intrinsic strength of monolayer graphene. Science. 2008;321(5887):385–388.
[11] Frank IW, Tanenbaum DM, van der Zande AM, et al. Mechanical properties of suspended graphene sheets. J Vac Sci Technol B Microelectron Nanometer Struct. 2007;25(6):2558.
[12] Cheng Z, Li Q, Li Z, et al. Suspended graphene sensors with improved signal and reduced noise. Nano Lett. 2010;10(5):1864–1868.
[13] Sidorenko A, Krupenkin T, Taylor A, et al. Reversible switching of hydrogel-actuated nanostructures into complex micropatterns. Science. 2007;315(5811):487–490.
[14] van der Zande AM, Barton RA, Alden JS, et al. Large-scale arrays of single-layer graphene resonators. Nano Lett. 2010;10(12):4869–4873.
[15] Chen C, Rosenblatt S, Bolotin KI, et al. Performance of monolayer graphene nanomechanical resonators with electrical readout. Nat Nanotechnol. 2009;4(12):861–867.
[16] Schedin F, Geim AK, Morozov SV, et al. Detection of individual gas molecules adsorbed on graphene. Nat Mater. 2007;6(9):652–655.
[17] Khan ZH, Kermany AR, Öchsner A, et al. Mechanical and electromechanical properties of graphene and their potential application in MEMS. J Phys Appl Phys. 2017;50(5):053003.
[18] Eom K, Park HS, Yoon DS, et al. Nanomechanical resonators and their applications in biological/chemical detection: nanomechanics principles. Phys Rep. 2011;503(4–5):115–163.
[19] Patel RN, Mathew JP, Borah A, et al. Low tension graphene drums for electromechanical pressure sensing. 2D Mater. 2016;3(1):011003.
[20] Du X, Skachko I, Barker A, et al. Approaching ballistic transport in suspended graphene. Nat Nanotechnol. 2008;3(8):491–495.
[21] Rickhaus P, Maurand R, Liu M-H, et al. Ballistic interferences in suspended graphene. Nat Commun. 2013;4:2342.
[22] Jang H, Park YJ, Chen X, et al. Graphene-based flexible and stretchable electronics. Adv Mater. 2016;28(22):4184–4202.
[23] Wang X, Shi G. Flexible graphene devices related to energy conversion and storage. Energy Env Sci. 2015;8(3):790–823.
[24] Köhler JM. Etching in microsystem technology. Weinheim (NY): Wiley-VCH; 1999. p. 368.
[25] Seidel H, Csepregi L, Heuberger A, et al. Anisotropic etching of crystalline silicon in alkaline solutions I. Orientation dependence and behavior of passivation layers. J Electrochem Soc. 1990;137(11):3612–3626.
[26] Sordan R, Miranda A, Traversi F, et al. Vertical arrays of nanofluidic channels fabricated without nanolithography. Lab Chip. 2009;9(11):1556.
[27] Dahiya R, Gottardi G, Laidani N. PDMS residues-free micro/macrostructures on flexible substrates. Microelectron Eng. 2015;136:57–62.
[28] Maji D, Lahiri SK, Das S. Study of hydrophilicity and stability of chemically modified PDMS surface using piranha and KOH solution. Surf Interface Anal. 2012;44(1):62–69.
[29] Samsure NA, Hashim NA, Nik Sulaiman NM, et al. Alkaline etching treatment of PVDF membrane for water filtration. RSC Adv. 2016;6(26):22153–22160.
[30] Chen Y, Zhang X, Zhang H, et al. High-performance supercapacitors based on a graphene–activated carbon composite prepared by chemical activation. RSC Adv. 2012;2(20):7747.
[31] Xu B, Yue S, Sui Z, et al. What is the choice for supercapacitors: graphene or graphene oxide? Energy Environ Sci. 2011;4(8):2826.
[32] Zhou M, Tian T, Li X, et al. Supercapacitance of chemically converted graphene with composite pores. Chem Phys Lett. 2013;581:64–69.
[33] Li Y, van Zijll M, Chiang S, et al. KOH modified graphene nanosheets for supercapacitor electrodes. J Power Sources. 2011;196(14):6003–6006.
[34] Nair RR, Blake P, Blake JR, et al. Graphene as a transparent conductive support for studying biological molecules

by transmission electron microscopy. Appl Phys Lett. 2010;97(15):153102.
[35] Kim YD, Kim H, Cho Y, et al. Bright visible light emission from graphene. Nat Nanotechnol. 2015;10(8):676–681.
[36] Miranda A, Halim J, Barsoum MW, et al. Electronic properties of freestanding $Ti_3C_2T_x$ MXene monolayers. Appl Phys Lett. 2016;108(3):033102.
[37] Sommer B, Sonntag J, Ganczarczyk A, et al. Electron-beam induced nano-etching of suspended graphene. Sci Rep. 2015;5:7781.
[38] Sonntag J, Kurzmann A, Geller M, et al. Giant magneto-photoelectric effect in suspended graphene. New J Phys. 2017;19:063028.
[39] Ferrari AC, Meyer JC, Scardaci V, et al. Raman spectrum of graphene and graphene layers. Phys Rev Lett. 2006;97(18):187401.
[40] Casiraghi C. Probing disorder and charged impurities in graphene by Raman spectroscopy. Phys Status Solidi RRL – Rapid Res Lett. 2009;3(6):175–177.
[41] Cançado LG, Jorio A, Ferreira EHM, et al. Quantifying defects in graphene via Raman spectroscopy at different excitation energies. Nano Lett. 2011;11(8):3190–3196.
[42] Ryu S, Maultzsch J, Han MY, et al. Raman spectroscopy of lithographically patterned graphene nanoribbons. ACS Nano. 2011;5(5):4123–4130.
[43] Yan J, Fuhrer MS. Correlated charged impurity scattering in graphene. Phys Rev Lett. 2011;107(20):206601.
[44] Chen J-H, Jang C, Adam S, et al. Charged-impurity scattering in graphene. Nat Phys. 2008;4(5):377–381.
[45] Moser J, Barreiro A, Bachtold A. Current-induced cleaning of graphene. Appl Phys Lett. 2007;91(16):163513.
[46] Dorgan VE, Behnam A, Conley HJ, et al. High-field electrical and thermal transport in suspended graphene. Nano Lett. 2013;13(10):4581–4586.
[47] Kim S, Nah J, Jo I, et al. Realization of a high mobility dual-gated graphene field-effect transistor with Al_2O_3 dielectric. Appl Phys Lett. 2009;94(6):062107.